

Vulcanian Eruptions

Amanda Bachtell Clarke

School of Earth and Space Exploration, Arizona State University, Tempe, AZ, USA

Tomaso Esposti Ongaro

Istituto Nazionale di Geofisica e Vulcanologia, Sezione di Pisa, Pisa, Italy

Alexander Belousov

Institute of Volcanology and Seismology, Petropavlovsk-Kamchatsky, Russia

Chapter Outline

1. Introduction	506	8. Vent Conditions	512
2. Hazards	506	9. Atmospheric Dynamics: Shock Waves	513
3. Field Example: Karymsky Volcano	507	10. Underexpanded Jet Stage	514
4. General Phenomenological Features of Vulcanian Eruptions	508	11. Plume Stage	515
5. Eruption Mechanism	509	12. Cyclic Activity, Transitions in Eruption Style	516
6. Eruption Initiation	510	13. Summary and Future Perspectives	517
7. Decompression and Fragmentation	511	Acknowledgments	518
		Further Reading	518

GLOSSARY

Adiabatic Flow An idealized flow condition in which heat does not enter or escape the fluid system due to perfect insulating boundaries.

Andesite An extrusive igneous rock type or magma of intermediate silica content falling between that of basalt and dacite; typically contains phenocrysts of plagioclase feldspar and pyroxene, and may contain hornblende depending on the water content of the magma.

Specific buoyancy flux The rate at which buoyancy per unit mass is injected into the atmosphere, expressed in terms of the volume flux and the density contrast between the injected fluid and the ambient fluid, such as the atmosphere. Buoyancy represents the force acting on an object or a parcel of fluid when it is immersed in a fluid with a different density and in a gravity field. Buoyancy is positive when the surrounding fluid has a higher density.

Country rock The rocks through which the magma travels on its way to the surface during eruption.

Dacite An extrusive igneous rock type or magma of intermediate silica content falling between that of andesite and rhyolite; typically contains phenocrysts of potassium feldspar and plagioclase feldspar, and may contain quartz, biotite, and hornblende.

Decompression wave This is a rarefaction wave. A continuous perturbation of a flow field generated by a pressure discontinuity,

traveling at the local speed of sound throughout the region at higher pressure.

Inviscid flow An idealized flow condition that assumes that the fluid involved has zero viscosity, and therefore loses no energy to viscous dissipation. The inviscid assumption is typically made when inertial forces far outweigh viscous forces.

Isothermal A fluid system is **isothermal** when its temperature (and the temperature of all its components) remains constant during motion or throughout the course of a thermodynamic transformation.

Juvenile A fragmented and solidified clast of erupted magma.

Lithic A dense pyroclast of solidified juvenile magma or an erupted fragment of country rock.

Specific momentum flux The rate at which momentum per unit mass is injected into the atmosphere, expressed in terms of the volume flux and the injection velocity.

Pseudofluid A fluid consisting of a mixture of at least two phases (solid, liquid, gas) that can be treated as a single fluid in which all phases have the same temperature and velocity.

Shock waves Waves characterized by a discontinuous change in pressure, density, temperature, and velocity, and by **supersonic** propagation velocities.

Self-similar solutions A solution of the equations of a dynamical system that has the same form (i.e., it is represented by the same function) at any point. Self-similarity usually allows a simple

parameterization of the dynamic variables in terms of constant scaling factors. For example, for jets and plumes, the scaling factor is the vertical distance from the source.

Speed of sound of a fluid The speed at which a pressure disturbance travels in a fluid.

Subsonic flow Flow of a fluid whose velocity always and everywhere remains less than that of the **speed of sound** in the fluid.

Supersonic flow Flow of a fluid whose velocity exceeds that of the speed of sound in the fluid.

Thermal Flow resulting from an instantaneous release of a buoyant fluid.

Vesicularity The volume fraction of bubbles in a magma or volcanic rock.

Volcanic bomb A fragment of magma or wall rock ejected by a volcanic explosion that is sufficiently large (formally >64 mm) to be transported in a ballistic trajectory. A **bread-crust bomb** is a volcanic bomb that in the process of transportation developed a specific surface texture resembling the cracked surface of a loaf of bread. This surface indicates that the interior of the magma fragment was still partially molten and continued to expand (due to the growth of gas bubbles) while its outer surface solidified and became brittle (chilled by ambient air).

1. INTRODUCTION

Since the early days of volcanology, classification of explosive activity has been based on the visual characteristics of eruption clouds. Modern investigations have demonstrated that, in most cases, visual qualitative differences between eruption clouds are closely related to fundamental differences in the eruption mechanisms, which, in turn, produce specific types of pyroclastic deposits recognizable in the field. Such links are rather straightforward for Hawaiian, Strombolian, Plinian, and Surtseyan types of explosive activity.

Vulcanian eruptions, however, are more complex to classify. Vulcanian eruptions were first distinguished by Mercalli and Silvestri (1891) who noticed that the 1888–1890 eruption of Vulcano in the Aeolian Islands was somewhat different from eruptions of nearby Stromboli volcano. Both volcanoes produced small to moderate scale, short-lived intermittent explosions, but explosions of Vulcano were louder, perhaps due to shock waves, eruption clouds were darker in color (almost black due to the presence of abundant ash), and ejected material had lower temperatures (few or no glowing ejecta were visible during daytime). The morphology of the juvenile products indicated higher viscosity and lower vesicularity magma at Vulcano; ballistics ranged from “bread-crust bombs” to dense, angular, glassy blocks. Mercalli thus suggested that Vulcanian activity is typical for magmas of intermediate composition.

Later investigations of other volcanoes have shown that visually similar “Vulcanian” eruptions can deposit very different pyroclastic products, and thus may have different eruptive mechanisms. Two major eruptive mechanisms

were suggested: phreatomagmatic and magmatic. Phreatomagmatic “Vulcanian” explosions commonly occur during initial “throat-clearing” and/or final stages of volcanic eruptions of other types, when rising/receding magma explosively interacts with groundwater or hydrothermal fluids surrounding the upper part of the conduit. Such explosions can be produced by magma of any composition (e.g., the 1924 eruption of Halemaumau crater in Hawaii was basaltic; Jaggar, 1947) and the resulting pyroclastic material contains a significant percentage of fragmented country rock.

However, in most cases (like the 1888–1890 classic eruption of Vulcano) there is no evidence of contact between magma and groundwater or hydrothermal fluids. Deposits of these eruptions contain few to no country rock fragments, and the participating magma is almost always of intermediate composition. Intermittent Vulcanian explosions of such eruptions commonly continue for months to years, sometimes with little variation in frequency and intensity. The mechanisms associated with such eruptions emphasize the critical role of a gas-impermeable plug composed of degassed, partly solidified magma that periodically forms in the upper part of a slowly ascending magma column. Volatiles gradually exsolve from crystallizing magma and accumulate as pressurized gas bubbles under the plug. Eventually the plug mechanically fails, initiating the eruption, and the released gas expands, fragmenting and ejecting magma of variable vesicularity.

Thus, currently the term “Vulcanian eruption” can be used in a broad sense, when dark intermittent “Vulcanian” clouds are observed irrespective of their eruptive mechanism (purely magmatic or phreatomagmatic), or in narrow sense, when such explosions are produced by the magmatic eruption mechanism. Here we consider only the purely magmatic mechanism of eruption initiation (see Chapter 30 for an account of phreatomagmatic mechanisms).

2. HAZARDS

Vulcanian explosions can precede large Plinian eruptions, as at Mt Pinatubo (Philippines; June 12–14, 1991); produce dangerous pyroclastic flows, as at Mount St Helens (USA; summer of 1980), and at Soufrière Hills volcano (Montserrat, BWI; July, August, and September of 1997); and present a significant hazard to aircraft, as at Galunggung (Indonesia) in 1982 and Redoubt (Alaska, USA) in 1989. At several volcanoes around the world, including Semeru (Indonesia), Sakurajima (Japan), and Karymsky (Russia), Vulcanian eruptions occur daily and can persist for years, potentially representing a large cumulative erupted mass. Ash and gases produced by Vulcanian eruptions are not typically ejected into the stratosphere where they would have a global effect; nevertheless explosion products can have devastating effects on local crops

and nearby populations. Vulcanian eruptions occur much more frequently around the world than Plinian eruptions offering excellent opportunity for detailed field observation. To date, however, such observations are rare in the literature. Continued observation of Vulcanian eruptions will play a critical role in advancing general theoretical understanding of explosive eruption dynamics.

3. FIELD EXAMPLE: KARYMSKY VOLCANO

Karymsky volcano is located in the eastern volcanic belt of Kamchatka Peninsula, Russian Far East. The cone-shaped stratovolcano (1553 m asl in 2010, 900 m above the base) of andesitic to dacitic composition occupies the central part of the 4.5-km-wide Karymsky caldera that formed 7700–7800BP (Braitseva and Melekestsev, 1991). Karymsky volcano is among the most active volcanoes in the world; it has had over 20 historical eruptive periods, 9 of which occurred in the twentieth century (Siebert and Simkin, 2002). Small to moderate scale short-lived Vulcanian

explosions with eruptive clouds 0.3–3-km high and a frequency of one every several minutes to every several days are characteristic of Karymsky's activity (Figure 28.1(A) and (B)). Concentrations of pyroclastic material in the eruptive clouds notably fluctuate; the weakest explosions produce light gray clouds containing few ash and ballistics, whereas the dark grey to black clouds of the strongest explosions are heavily ash laden and commonly accompanied by small-volume hot avalanches originating from abundant ballistic fallout (Figure 28.1(D)). Relatively uniform explosions with regular repose intervals that commonly span over periods of days to months gradually change their average intensity and frequency (Figure 28.1(A) and (B)). Some periods of explosive activity are combined with the extrusion of small intra-crater domes and/or viscous blocky lava flows up to 20–30-m thick, with the explosions completely or partially destroying these domes/flows. Products of the explosions are bread-crust bombs (Figure 28.1(E)), as well as lapilli and ash composed of poorly vesiculated blocky particles (Figure 28.1(F)).

Investigations of paleosol sections have shown that periods of long-lasting Vulcanian activity were common

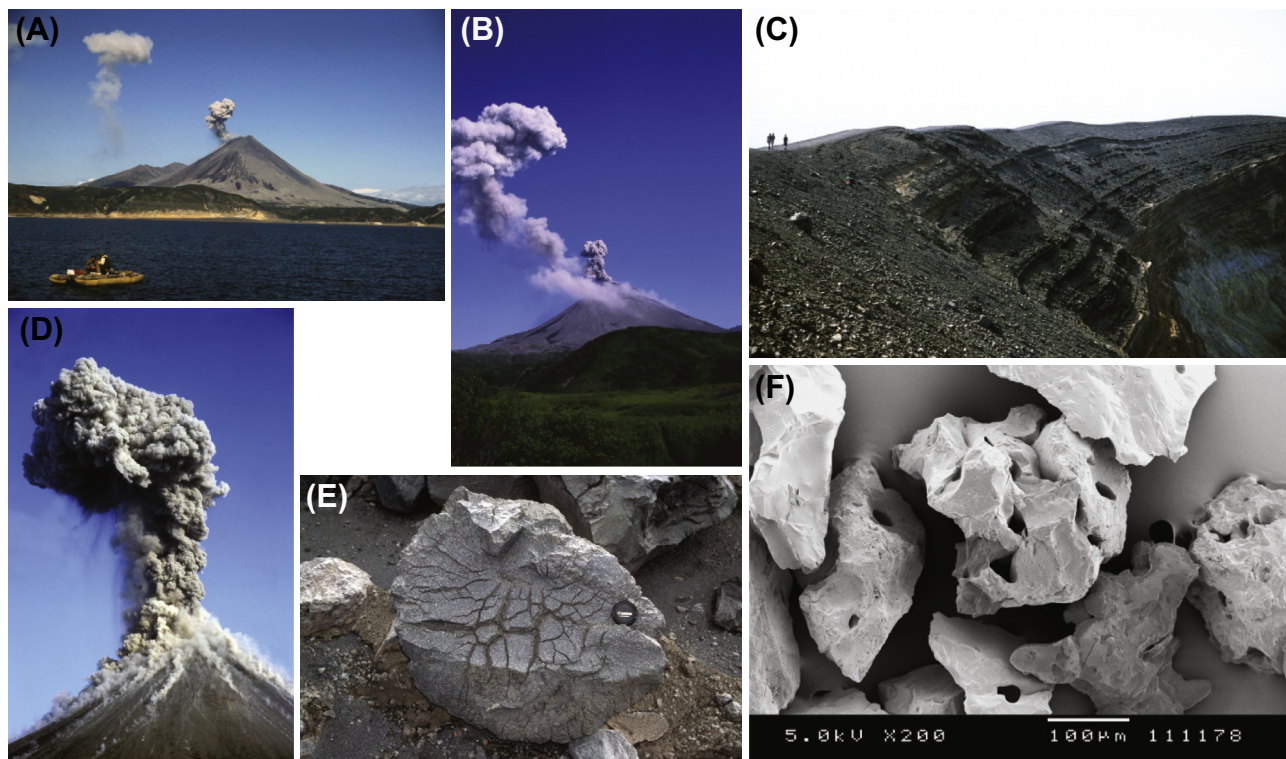


FIGURE 28.1 A) 1996 and (B) 2005 eruptions of Karymsky volcano. These consisted of frequent moderately strong explosions with few ballistics. Eruption cloud is approximately 1 km above the crater. Eruption clouds of previous explosions that occurred minutes before are drifting downwind; (C) Inner slope of the crater of Vulcano, Aeolian Islands, Italy. Multiple layers of bombs and lapilli were deposited by numerous transient explosions of the 1888–1890 eruptions; (D) Strongest Vulcanian-type explosions of Karymsky volcano, July 2004. Quickly rising eruption cloud is more than 1 km above the vent. Final height of the eruption cloud will be approximately 3 km. Massive ballistic fallout forms multiple hot avalanches on the volcano slope. A curtain of ash fallout is visible on the lee side of the eruption cloud; (E) Bread-crust bomb of Karymsky volcano, 1999. Lens cap is 6 cm across; (F) Scanning electron microscope image of ash particles of Karymsky volcano eruptions in 2003. Blocky sharp-edged particles with no/few gas bubbles indicate fragmentation of degassed highly viscous magma. All photos by A. Belousov.

throughout the 5000 years of history of the stratovolcano; such periods are indicated in paleosols by high concentrations of dispersed fine-grained ash. The last eruption cycle of Vulcanian activity started at Karymsky in 1996 and continues today. Intensity of the eruptions has fluctuated through time: periods were characterized by either pure explosive activity of varying intensity or by explosions associated with lava extrusions; also there were several episodes of complete inactivity that lasted up to several months.

As an example we present a description of the volcano's activity in July 2008. The explosions were associated with the slow extrusion of a small andesitic lava dome in the summit crater, and were separated by periods of vigorous gas venting (in the form of a continuous vertical white plume with an audible "jet engine" sound) from the dome apex. The gas venting ceased abruptly several tens of minutes before each explosion indicating plugging and pressurization of the magma conduit. Each explosion started with a sudden violent ash-and-ballistic-rich loud outburst, commonly consisting of a rapid succession of several inclined jets. Minutes-long pulsatory expulsions of ash clouds of declining intensity and ash concentration followed this initial stage, generating ash plumes up to 3 km above the crater. All of the observed explosions produced large volumes of ballistic materials that landed on the upper flanks of the volcano, although the specific volume varied from event to event (up to several tens of thousands of cubic meters per explosion). Massive ballistic fallout from the largest explosions produced small hot avalanches on the volcano slopes (Figure 28.1(D)). No incandescence was visible during daylight hours and dull red ballistics were observed during the night. Ejected pyroclasts indicate that the fragmenting andesitic magma was represented by two end members: vesicular with large irregular interconnected gas bubbles (vesicularity 40%), and dense with small isolated gas bubbles (vesicularity 5%).

4. GENERAL PHENOMENOLOGICAL FEATURES OF VULCANIAN ERUPTIONS

Vulcanian eruptions may have a wide range of dispersal areas and degrees of fragmentation, making them difficult to classify from deposit characteristics alone. For example, Walker (1973) proposed in a preliminary sense that Vulcanian eruptions may have dispersal areas similar to those of subplinian eruptions, but should contain a larger proportion of fine-grained pyroclasts (Figure 28.2). This increased "explosivity" of Vulcanian eruptions reflects dynamic factors (i.e., it is not related solely to rheological or compositional differences), and was attributed in particular to plugging of the vent. Additional synthesis of field data by Cas and Wright (1987) demonstrates that

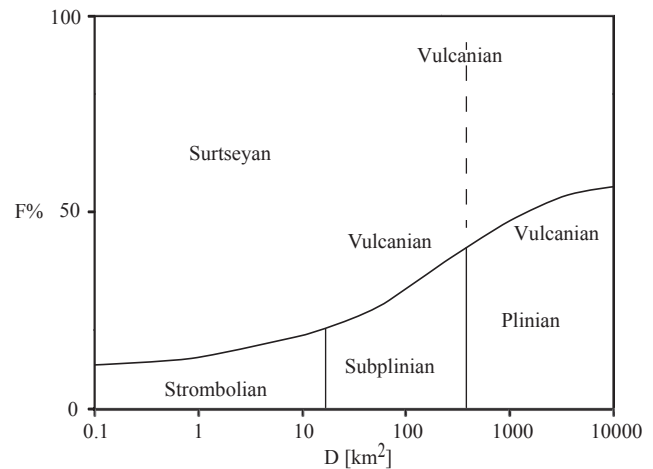


FIGURE 28.2 Classification of Vulcanian eruptions in terms of the percentage of (vertical axis) clasts <1 mm in diameter on the main dispersal axis where it crosses the isopach of thickness equal to 10% of the maximum thickness of the deposit (F%), and (horizontal axis) the area enclosed by the same isopach (D). Data defining the Vulcanian fields are from Wright et al. (1980), based on eruptions of Cerro Negro (Guatemala, 1968 and 1971), Fuego (Guatemala, 1971), Ngauruhoe (New Zealand, 1974 and 1975), Mt Edgemont (New Zealand, 1665), and Irazu (Costa Rica, 1963). Modified from Walker (1973) and Cas and Wright (1986).

Vulcanian eruptions equal subplinian to Plinian in terms of dispersal areas, but almost always contain a larger proportion of fine-grained pyroclasts, sometimes significantly more (Figure 28.2).

However, Vulcanian eruptions share some common observable phenomenologies that make them identifiable.

- Distinctive deposit characteristics
 - *Relatively small magnitude.* The juvenile mass erupted in a single Vulcanian event does not usually exceed that stored in the conduit, and is not typically greater than 10^{11} kg (VEI 3–4). However, cyclic activity may result in much larger cumulative erupted volumes, producing thick coarsely layered deposits proximal to the vent (Figure 28.1(C)).
 - *Relatively fine ejecta.* With respect to other explosive eruptions with similar volumes and dispersal areas, the average mean particle size of Vulcanian eruptions is relatively fine (Figure 28.2). This phenomenon is explained by the higher specific energy related to the initial rapid decompression stage.
 - *Low-vesicularity pyroclasts.* The average vesicularity of pyroclasts is lower (and bubble walls are thicker) than those typical of other types of magmatic eruptions (Figure 28.1(F)).
 - *Variable clast vesicularity.* It testifies to the progressive sampling of variably vesiculated conduit magma by the deepening fragmentation wave.
 - *Blocky shape of ash particles.* It indicates brittle fragmentation of highly viscous magma (Figure 28.1(F)).

- **Strong ballistic ejection.** Large numbers of decimeter-to meter-sized clasts are generated by explosive plug disruption. Typically, ballistics are bread-crust bombs composed mostly of poorly vesiculated and degassed magma ejected in an almost solid state, representing the plug material (Figure 28.1(E)). Ballistics are common for other eruption types as well, but they are different in notable ways; they are either more vesicular in Plinian and Strombolian eruptions, consisting of large pumice or scoria clasts, or less vesicular in phreatic or phreatomagmatic eruptions, dominated by lithic country rocks. Unusually large ballistic ranges in Vulcanian explosions can be caused by the cumulative effect of a strong initial pressure gradient and the accelerating drag of the ejected pyroclastic mixture.
- **Transient behavior.** Vulcanian eruption duration is limited, such that the injection lasts seconds to minutes (Figure 28.1(A) and (B)). Vulcanian eruptions often serve as the opening stage for some subplinian or Plinian eruptions.
- **Supersonic regimes.** Vulcanian explosions are distinguishable by a leading shock wave and subsequent formation of an underexpanded jet. This stage can be recognized by infrasonic and acoustic measurements. The transient injection and the underexpanded jet lead to the typical “mushroom” shape of the jet immediately above the vent (Figure 28.1(A), (B) and (D)).
- **Short-lived atmospheric plume.** The evolution of the volcanic plume is controlled by the large vortex structure at its head, which controls atmospheric air entrainment and also partly explains the typical “mushroom” shape (Figure 28.1(A), (B) and (D)). As a consequence, ascent velocity of the plume follows a different temporal evolution than a steady, sustained plume.

Despite these common features, the wide range of variability of eruptive conditions makes a simply phenomenological definition of Vulcanian eruptions not fully satisfactory. We therefore proceed by defining Vulcanian eruptions from a dynamical point of view.

5. ERUPTION MECHANISM

Vulcanian eruptions result from the sudden decompression of a volcanic conduit that contains highly pressurized crystallized bubbly magma of intermediate composition (Figure 28.3). These eruptions initiate when a conduit plug or dome is disrupted due to a sufficiently high pressure gradient in the underlying magma. Upon plug disruption, a decompression wave, followed by a fragmentation front, travels down the conduit, while a compression shock propagates into the atmosphere. At the fragmentation front, vesicular magma is disrupted into a gas–pyroclast mixture,

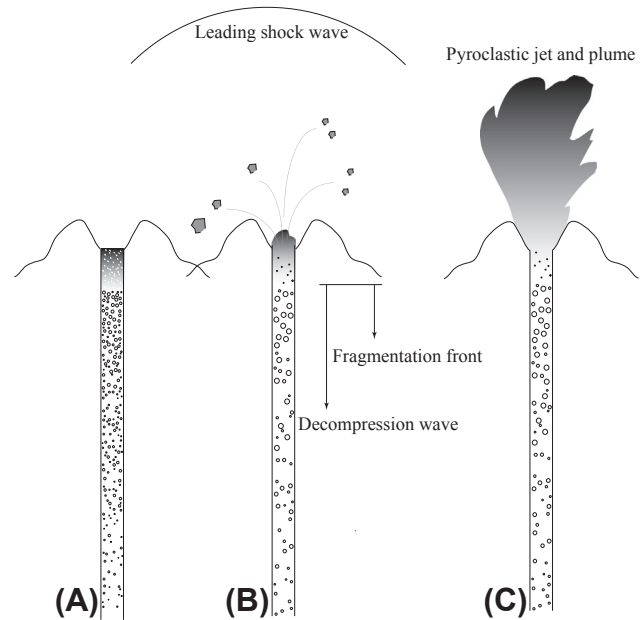


FIGURE 28.3 Vulcanian Eruption Schematic. (A) A dense plug seals a conduit containing bubble-bearing magma. (B) Eruptions initiate when the plug is disrupted, evidenced by the launching of ballistic clasts. A decompression wave, followed by a fragmentation wave, travels into the conduit, while shock waves propagate through the atmosphere. (C) An overpressured mixture of fragmented magma and expanding gas is ejected into the atmosphere.

propelled upward, and ejected from the vent into the atmosphere as an underexpanded jet at sonic to supersonic velocities. This ejection is characteristically impulsive and unsteady. Transition to the subsonic regime can occur very rapidly above the vent, so that the jet may evolve into a buoyant plume, collapse gravitationally to form pyroclastic density currents, or both may occur simultaneously.

Typically, only a portion of the magma in the conduit is fragmented and evacuated, such that Vulcanian eruptions characteristically are of relatively small volume and last only seconds to minutes. They may occur as single events or as a sequence of explosions spaced sufficiently far apart in time to produce distinguishable, discrete, unsteady events.

The short duration and unsteady vent conditions of Vulcanian eruptions define them and make them distinct from quasi-steady Plinian, subplinian, or Hawaiian eruptions, for which it is generally assumed that bubbly magma rises to meet the fragmentation front and thus steadily feeds vent flux over hours to days. Strombolian activity can also be characterized as short-lived and impulsive, however, in Vulcanian events bubbles cannot ascend quickly through the highly viscous magma as they do at Stromboli, making the dynamics significantly different. Column heights typically exceed heights associated with Strombolian eruptions (see Chapter 27) and are less than those associated with Plinian and subplinian eruptions (see Chapter 29).

6. ERUPTION INITIATION

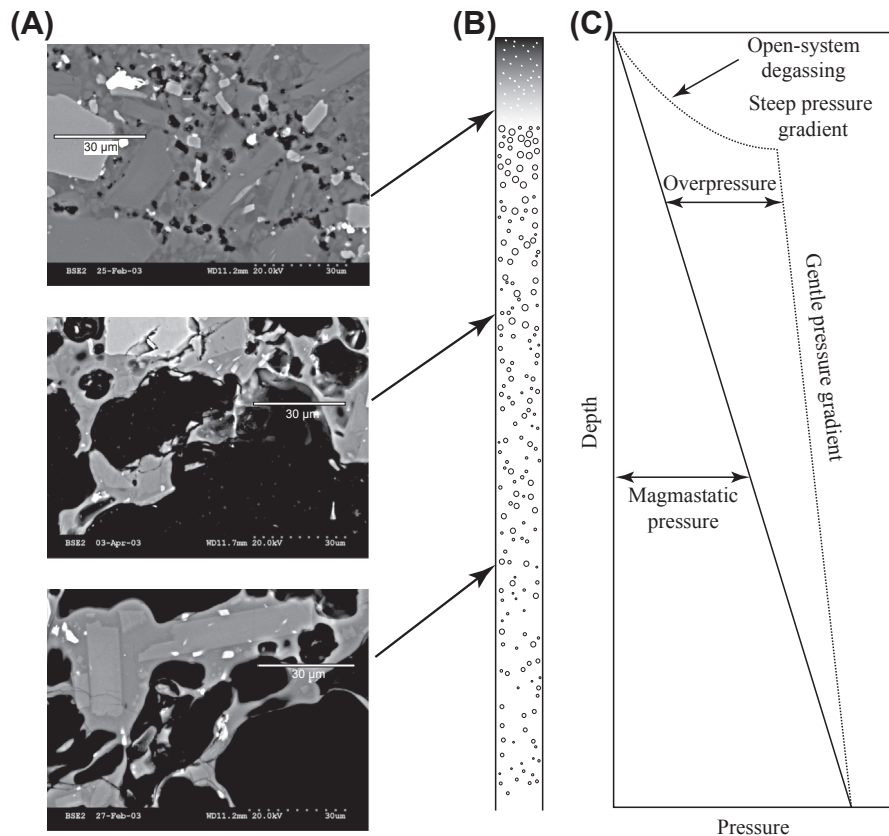
Vulcanian eruptions initiate when a coherent magma plug or dome that sealed the conduit is suddenly disrupted. Observational evidence of this initiation process consists of the formation of crystallized and degassed domes, ballistic clasts launched at the very beginning of an eruption, and dense ballistic clasts in deposits. Plug disruption occurs when pressure in the underlying conduit rises sufficiently (up to 10–15 MPa, but usually <5 MPa, based on the strength of typical magmas) to exceed the mechanical strength of the lava or when the overlying dome collapses. Two key processes are involved in creating conduit plugs: magma outgassing and subsequent microlite crystallization in the volcanic conduit. As magma rises water exsolves from the melt in response to decreasing pressure, and a corresponding shift in the liquidus causes anhydrous phases to crystallize, especially plagioclase feldspar. Crystallization and degassing increase magma viscosity and, by concentrating volatiles in the remaining melt, force further degassing. Bubble connections develop at some threshold vesicularity. Simultaneous crystallization and degassing tends to concentrate vesicles in the interstices between crystals, and may enhance permeable gas loss via connected bubble networks. The consequent outgassing may cause

vesicle collapse and formation of a dense viscous plug that leads to the stagnation of underlying magma (Figure 28.4).

Many of these same processes lead to increased pressure below the viscous plug. For example, magma pressure may increase due to rheological stiffening of the ascending magma (Figure 28.4) and volatile pressure may increase because bubble growth is inhibited by high viscosity. Eventually pressures reach values sufficient to disrupt the overlying plug resulting in fragmentation of both the plug and underlying magma (Figure 28.3(B)).

Ballistic blocks or bombs mainly represent the disrupted sealing plug. Although ballistic block fields have been documented carefully for several types of eruptions (including the 1977 phreatomagmatic eruptions of Ukinrek Maars, Alaska, the 1992 subplinian eruptions of Crater Peak Vent, Mount Spurr volcano, Alaska, the 1997 Vulcanian eruptions of Soufrière Hills volcano, and the 1999 Vulcanian eruptions of Guagua Pichincha volcano, Ecuador, among others) ballistic launch in Vulcanian eruptions (or in the Vulcanian stage of complex eruptive sequences) is particularly intense and characterized by unusually large ranges. Blocks on the order of a half meter in diameter can be launched to 3 km from the vent, and in some cases smaller blocks can reach >6 km from the vent.

FIGURE 28.4 Schematic representation of conduit conditions prior to Vulcanian eruptions. (A) SEM images of pyroclasts from Soufrière Hills volcano, in which bubbles (black) and crystals (white and light gray) can be distinguished from rapidly quenched melt (glass, darker gray). (B) Relative vertical source positions in the conduit for each sample are indicated by arrows pointed at the conduit schematic. (C) The pressure profile for the bubbly magma in an unplugged state (magmastatic) and a preeruption overpressured state. Modified from Clarke *et al.* (2007).



They may exhibit a bread-crust texture indicating that interior gas expanded after the surface was quenched. In general, ballistic size decreases with distance from the vent. However, in some cases the opposite is true because complex drag interactions between the blocks and the expanding pyroclastic mixture and the surrounding air lead to very high drag-to-weight ratios for some small blocks.

Observations and numerical models resolving the full Lagrangian equations for individual particles have shown that, in Vulcanian eruptions, clast trajectories quite often deviate from parabolic trajectories. In particular, accelerating drag exerted by the starting jet and the added effect of a strong pressure gradient lead to launch distances up to 70% greater than those predicted by a simple ballistic analysis (Figure 28.5).

7. DECOMPRESSION AND FRAGMENTATION

Upon plug disruption, a decompression wave travels at the local sound speed into the conduit (Figure 28.3(B)). The decompression wave is followed by a fragmentation wave that travels more slowly than the pressure wave through the

bubbly magma (Figure 28.3(B)). The mathematical formulation of such a model is analogous to that for flow in a one-dimensional shock tube. In this configuration, a one-dimensional tube is subdivided into a high-pressure region at the base of the tube and a low-pressure region in the upper portion, separated by a diaphragm. Upon rupture of the separating diaphragm, a compression wave (shock) propagates upward, while a rarefaction wave decompresses the underlying fluid.

Behind the fragmentation front, a mixture of expanding gases and freshly produced pyroclasts is projected upward and expelled from the volcanic vent. The fragmentation wave is generally thought to fragment and quench the magma faster than dissolved gases can exsolve in response to the decompression. Therefore, to first order, exsolution of magmatic volatiles is assumed to be insignificant during the decompression and fragmentation process, and thus only previously exsolved volatiles participate in the eruption. Eruptive products therefore preserve to some extent the preexplosion state of magma vesiculation. However, up to several percent by volume bubble expansion can occur during eruption, due to bubble growth, and thus erupted clasts may be more vesicular than the preeruptive magma. The velocity of the fragmentation wave is thought to

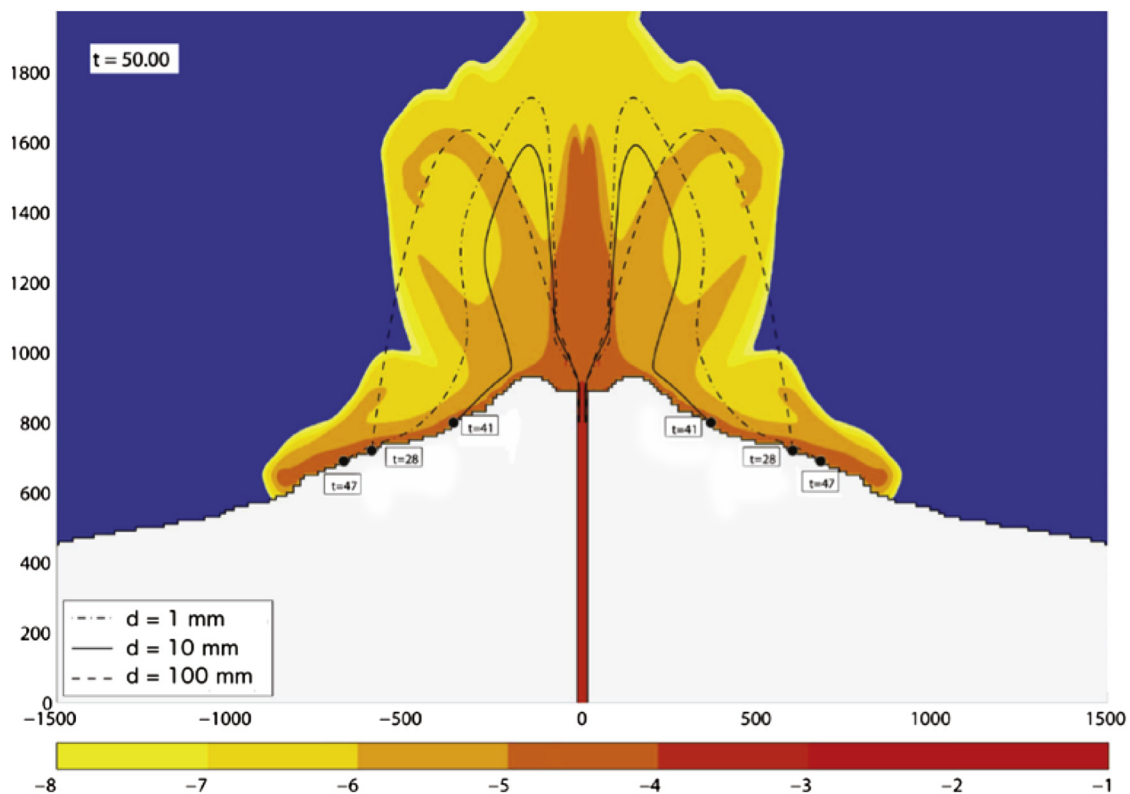


FIGURE 28.5 Computed trajectories and flight times of three different sets of particles based on the 1997 eruption of Soufrière Hills volcano, Montserrat. Vertical and horizontal scales in are in meters; the color scale represents particle volume fraction in \log_{10} scale (unitless); travel time labels are given in seconds. Lines indicate trajectories for different particle diameters (d). Note that the ballistics have been influenced to varying degrees by the dynamics of the modeled pyroclastic jet. *Modified from de' Michieli Vitturi et al. (2010).*

greatly exceed magma ascent velocity, and the magma is assumed to have stagnated prior to fragmentation. Therefore the fragmentation front meets magma with varying degrees of crystallinity, vesicularity, and viscosity. The observed variability of pyroclast densities and crystallinities in Vulcanian deposits supports this concept of a progressive downward-migrating fragmentation front.

The details of the fragmentation process remain a subject of active research in volcanology, but several models have been presented. Fragmentation is thought to occur due to high shear or elongational strain rates, high tensile stresses at bubble walls due to overpressured bubbles, or a combination of the two. When magma is subject to very high strain rates its characteristic relaxation time may exceed the time over which stresses are applied, preventing the magma from stretching or flowing, leading to brittle behavior and fragmentation. Magma relaxation time increases with magma viscosity, meaning that fragmentation generally occurs more readily in higher viscosity magmas. The tensile stress threshold may be exceeded in bubbly magma when the stress on bubble walls exceeds the tensile strength of the magma. Fragmentation due to this condition is thought to occur by disruption of bubbles near the free surface of a vesicular magma, where there can be a significant pressure gradient between the ambient pressure and the bubble gas pressure. According to a series of numerical solutions and experiments on natural melts, bubbles should stop growing long before explosive fragmentation, primarily because of increasing melt viscosity. These solutions led to the concept that bubble volume fraction never exceeds 66–83% vesicularity. This range of vesicularity is often used as a fragmentation criterion in numerical models of magma ascent.

It is likely that each of these mechanisms contributes to fragmentation in Vulcanian eruptions. Upon plug disruption, and decompression of the underlying bubbly magma, one or both of the strain rate thresholds may be exceeded due to magma acceleration in response to the sudden decompression. The decompression also leads to rapid bubble expansion, which should produce very high strain rates within bubble walls such that bubble walls behave as a brittle solid and interbubble partitions are ruptured instead of stretched. The tensile stress criterion may also apply because plug disruption suddenly exposes the underlying magma to a very low ambient pressure, which rapidly increases bubble overpressure and thus the magma exceeds the threshold overpressure criterion. In some cases, upon plug disruption, the volume fraction criterion may be reached as bubbles expand in response to the decompression.

Laboratory experiments have been used to test fragmentation theories regarding the nearly instantaneous decompression of vesiculated magma under conditions appropriate for Vulcanian eruptions, as described above. The magnitude of the pressure drop and the vesicularity

were varied in order to define a fragmentation threshold. According to results, the minimum required pressure drop varies linearly with the effective tensile strength of the magma (~ 1 MPa) and is inversely proportional to the vesicularity.

This relationship holds for a wide range of magma compositions, crystallinities, and porosities. An interesting point to note is that for magmas with $>20\%$ vesicularity, a sudden decompression of magnitude 5 MPa results in fragmentation, whereas low vesicularity magmas ($\leq 10\%$ vesicularity) may require a drop in excess of 15–30 MPa.

Experiments have also shown that onset of permeability may relieve bubble pressure during propagation of a fragmentation wave (syn-fragmentation) by allowing high-pressure volatiles to escape via connected bubble pathways in magma below the fragmentation front, thus increasing the fragmentation threshold.

The corresponding propagation speed of the fragmentation front, as measured experimentally, generally falls between 2 and 70 m s^{-1} for magmas with 20–60% vesicularity and increases roughly linearly with the magnitude of the sudden decompression. Vulcanian explosions stop when the decompression front reaches unfragmentable magma, which may occur when the front reaches a depth in the conduit where: (1) the magma has insufficient vesicularity; (2) the bubbles are insufficiently overpressured; (3) the magma has sufficiently low viscosity allowing it to respond quickly to high strain rates; or (4) the front has weakened such that the pressure gradient is below the fragmentation threshold.

8. VENT CONDITIONS

The vent flux associated with Vulcanian eruptions is highly impulsive because the eruptions represent the rapid discharge of magma from a pressurized conduit of finite volume. Initially, the flux rapidly increases, then may become steady for a relatively short period, and then quickly wanes. When the fragmentation wave reaches unfragmentable magma the conduit is fully depressurized, and the vent flux decays to near zero, although sustained gas exhalations following the main pulse have been documented for several eruptions.

The motion of the fragmented pyroclast/gas mixture at the vent can be calculated by assuming that, upon decompression, available gas in the underlying magma expands to atmospheric pressure as an ideal gas and accelerates the pyroclasts to the same velocity as the gas itself (pseudofluid approximation). The mixture of pyroclasts and gas is assumed to be isothermal when heat is transferred from the clasts to the gas on timescales much shorter than the duration of the explosion. This assumption applies when the average diameter of pyroclasts is $\ll 1$ mm. Solutions for a wide range of initial gas mass fractions (0.01–0.1), initial

temperatures (600–1400 K), and initial pressure ratios across the plug (0–100) reveal several trends (some shown in Figure 28.6): vent velocity increases nonlinearly with increasing pressure ratio and increasing volatile mass fraction; mass flux normalized by conduit/vent size increases with increasing pressure ratio due to a rise in vent velocity and decreases with increasing volatile mass fraction due to a decline in mixture density.

The isothermal assumption is not appropriate when a significant portion of the pyroclasts are $> \sim 1$ mm. Mixture velocity decreases and mixture density increases with increasing levels of thermal disequilibrium associated with increasing proportions of large clasts (Figure 28.6). These lower vent velocities may push the system toward gravitational collapse and formation of pyroclastic density currents.

A more complete description of the flow conditions leading to the development of Vulcanian eruptions comes from the multidimensional solution of the nonequilibrium, multiphase flow equations for a mixture of expanding gas and pyroclasts in the atmosphere. On exiting from the vent, the expansion fan radiates as a three-dimensional wave. Analogous to a flow exiting a supersonic nozzle, velocity at the vent cannot exceed the speed of sound in the multiphase mixture and the subsequent expansion in the atmosphere leads to a complex three-dimensional shock wave pattern. Applications to the eruptive conditions at Soufrière Hills volcano have shown that flow at the conduit exit was likely characterized by a stage of (unsteady) sonic to supersonic flow conditions lasting up to about 30 s, with vertical velocities above the vent slightly exceeding the sound speed in an equivalent pseudofluid mixture and higher-than-atmospheric pressure (with pressure ratio as high as 40, Figure 28.7). The initial overpressured jet stage was then followed by a later stage of subsonic flow and decreased mass flow rate, corresponding in time to column collapse and the formation of pyroclastic density currents.

9. ATMOSPHERIC DYNAMICS: SHOCK WAVES

Shock waves propagating ahead of the pyroclastic mixture have been documented during many Vulcanian eruptions, and are referred to as leading shock waves. They have been observed at, for instance, Sakurajima volcano, Japan (Ishihara 1985), and Mt Ngauruhoe in New Zealand (Self et al. 1979). These shock waves result from the initial pressure difference between the high-pressure, gas-rich magma in the conduit and the atmosphere, which, up until the moment of eruption initiation, are separated by the conduit plug. These waves represent a pressure, temperature, and density discontinuity and travel at sonic to supersonic speeds ahead of the pyroclastic mixture. Leading shock waves are sometimes visible because they condense atmospheric water vapor, allowing their velocities to be estimated. The passing of one of these shock waves is marked by an N-shaped pressure variation in time, in which a sharp increase in atmospheric pressure is followed by a dip to a pressure that is less than atmospheric, followed by a return to atmospheric pressure. These N-shaped waves have been documented by stationary pressure sensors at several volcanoes.

For the simple case of adiabatic and inviscid flow of an ideal gas, shock characteristics have been derived in terms of the preexplosion pressure ratio across the plug by solving the conservation of mass, momentum, and energy equations over a control volume that encompasses and travels along with the shock wave. Note that this control volume considers only two pressures that represent a single pressure above and a single pressure below the plug, and does not consider vertical or horizontal variations in pressure nor pressure differences between phases that may occur in a volcanic conduit. Solutions show that, at a given distance, the velocity and amplitude of the wave, or the strength of the shock defined as the ratio of pressure before,

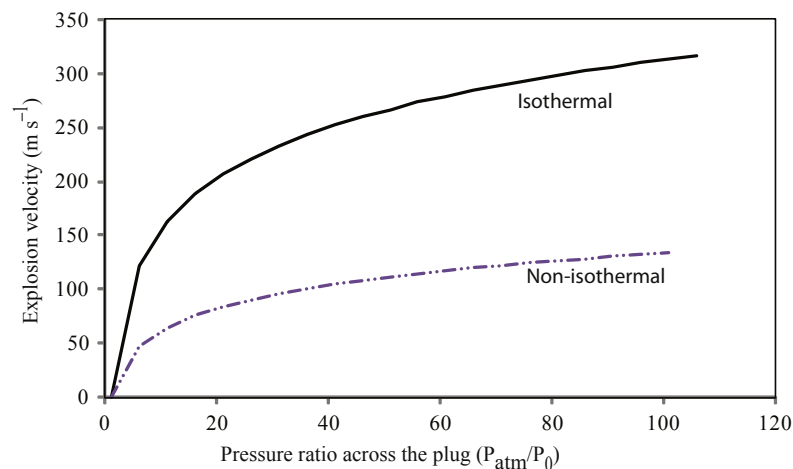


FIGURE 28.6 Calculated vent velocities for a range of initial pressure ratios, using a form of the shock tube equations for isothermal and nonisothermal cases. The nonisothermal solutions assume 0.01 mass fraction volatiles at 1000 K (dashed–dotted line) and account for 3% of particles > 1 mm in diameter. The isothermal solutions (solid black line, also for 0.01 mass fraction volatiles and initial temperature of 1000 K) significantly exceed the nonisothermal solutions.

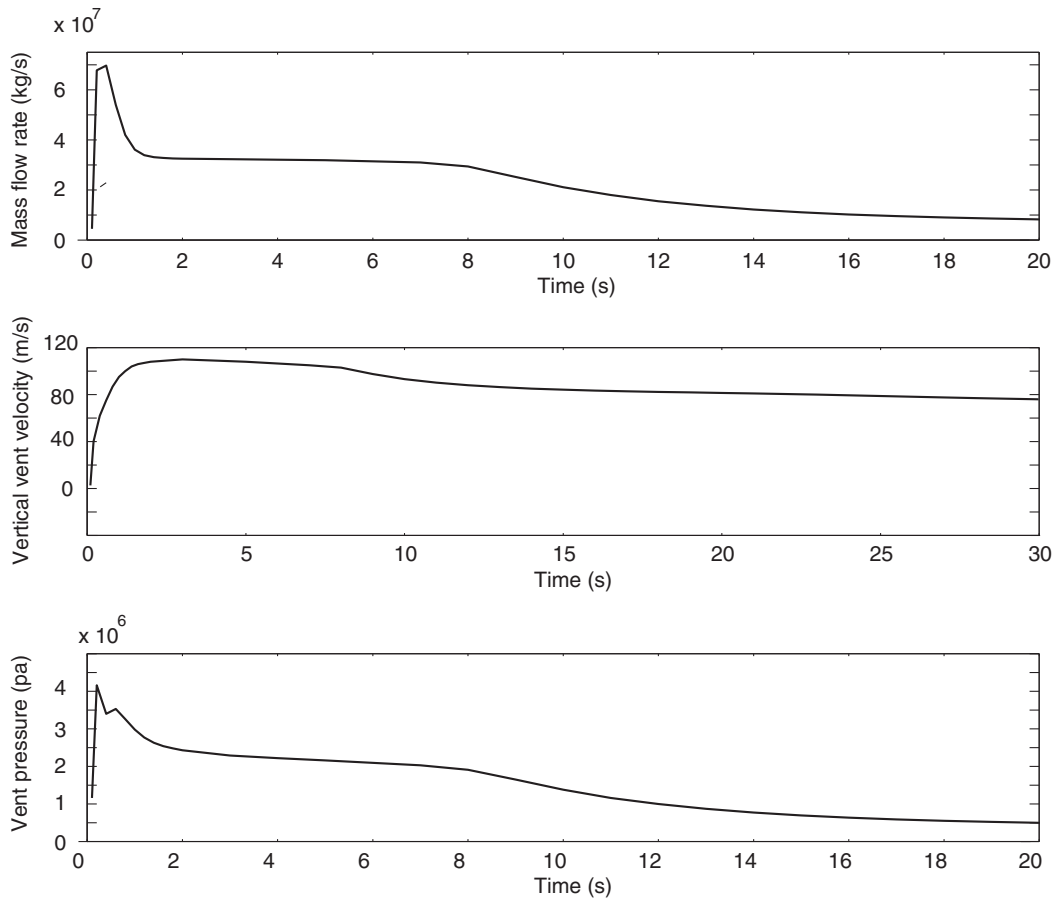


FIGURE 28.7 Vent conditions calculated by multiphase simulations of the 1997 Vulcanian eruptions of Soufrière Hills volcano, Montserrat. Note that the mass flow rate reaches nearly 10^8 kg s^{-1} for less than 2 s, and then declines to a nearly constant rate of $3 \times 10^7 \text{ kg s}^{-1}$ for 10 s before tapering to very low values. Mixture velocity above the vent is supersonic for 10 s (using a calculated sound speed for the pyroclastic mixture of 100 m s^{-1}) and remains nearly constant for 10 s of seconds. The vent pressure is in excess of 20 times atmospheric pressure for the first 8 s of the event and remains overpressured for the first 20 s of the event. Modified from Clarke *et al.* (2002b).

to pressure after the wave, decay nonlinearly with decreasing initial pressure ratio across the plug.

Recent experimental and numerical work shows that, in Vulcanian eruptions, the presence of the particulate phase tends to reduce the velocity and strength of shock waves relative to those formed by single gas phases. This trend is in part due to the fact that, generally speaking, the shock wave is formed by the expanding gas alone, and particles hinder gas expansion by reducing the gas volume and hinder gas motion via an interphase drag force. The magnitude of this reduction is independent of particle size, although particle volume fraction is important; shock speed and strength decrease with decreasing gas volume fraction.

Shock waves generated at Sakurajima volcano moved with velocities of $440\text{--}500 \text{ m s}^{-1}$ according to high-speed video observations; experiments suggest corresponding preexplosion conduit pressures of 1.5–10 MPa, which compares reasonably well with values of 0.2–5 MPa calculated using a numerical approach using recorded shock wave strength.

10. UNDEREXPANDED JET STAGE

Because Vulcanian eruptions initiate via a sudden decompression of a high-pressure bubbly magma, the resulting pyroclastic mixture may enter the atmosphere at supersonic velocities and in an overpressured state. Evidence of higher-than-atmospheric pressure at the conduit exit and of sudden-onset impulsive source is provided by empirical and theoretical analysis of the shape of volcanic jets (stalks with nearly vertical edges, rather than conical stems, and a large vortex front—“mushroom shape”), as well as from infrasonic and acoustic measurements of shock waves. As a consequence, the erupting mixture must equilibrate to the ambient pressure through gas decompression and expansion. The decompression of the gas–particle mixture is a complex nonlinear process, which is affected by the conduit flow and fragmentation dynamics and by the shape of the volcanic crater, among other factors.

To understand the decompression process further, we can apply scaling relationships derived from experiments on

unsteady underexpanded jets of gases having thermodynamic properties similar to those of a gas–particle mixture (Orescanin et al., 2010). For initial conduit pressures of 15 MPa (pressure ratio of ~ 150), fluid properties of dilute gas–particle mixtures, and conduit diameters ~ 30 m, it is found that Vulcanian jets should equilibrate to atmospheric pressure at a distance of about 240 m from the source. At lower pressure ratios ($K \sim 5$) the jet decompresses within the first 50 m above the vent. Mixture density decreases during the decompression and expansion stage, however, its value at atmospheric pressure may still exceed that of the ambient fluid. The subsequent transition to a buoyant plume is then controlled by the rate at which air is mixed into the jet.

The combination of field observations from Soufrière Hills volcano, and multiphase flow models for gas–particle mixtures shows that pressure inside the volcanic jets might have adjusted to atmospheric pressure within about 200 m from the vent, but transient vent conditions significantly affected the stability properties of the jet, which collapsed generating radially spreading pyroclastic density currents.

11. PLUME STAGE

Above the jet expansion region, at subsonic velocity, compressibility can largely be neglected and the dynamics of Vulcanian eruptions are dominated by the balance between specific momentum flux $\dot{M} = \frac{\beta}{\alpha} R^2 U^2$ and specific buoyancy flux $\dot{B} = g \left(\frac{\beta - \alpha}{\alpha} \right) R^2 U$. Here β indicates the eruptive mixture density, α the atmospheric density, g the gravitational acceleration, R the plume radius, and U its average vertical velocity. For stationary turbulent plumes, the Morton length scale $L = \frac{M^{3/4}}{B^{1/2}}$ characterizes the transition between momentum- (*jet*) and buoyancy-dominated (*plume*) regimes. Experimental and theoretical results predict a buoyancy-dominated regime above a height of about $5L$ from the vent.

For several different unsteady vent conditions, similarity solutions of the fluid dynamics equations are possible for Vulcanian jets and plumes. Depending on the duration of the injection with respect to the plume ascent time, Vulcanian eruptions can either be described as thermals (when the timescale of release is much less than the timescale of flow propagation) or short-lived releases of buoyancy and momentum. Vertical motion of a thermal is controlled entirely by the total buoyancy injected (B). Thermals commonly have spherical morphology and resemble a spherical vortex in which flow is nonuniform, with upflow in the center and downflow at the edges. The vertical velocity of a thermal decreases linearly as the height above the source increases, and decreases with the square root of time after the release ($U \sim t^{-1/2}$). Thermals

are low-energy, very small volume, end members of Vulcanian eruptions and have been observed at Fuego in Guatemala, as well as during the 1982 eruption of Sakurajima volcano, Japan (Figure 28.8).

Short-lived jets characterize more energetic Vulcanian eruptions. In such cases, throughout most of the flow, the vertical velocity of the flow front decreases with time raised to the $3/4$ power ($U \sim t^{-3/4}$). This scaling breaks down far from source, where atmospheric stratification plays a dominant role in the ascent dynamics. The well-documented 1975 eruptions of Ngauruhoe appear to have been dominated by momentum forces (Figure 28.8). Still other eruptions are best explained by a short injection of both momentum and buoyancy. These eruptions exhibit more rapid deceleration than either a purely buoyant thermal or a purely momentum-driven unsteady jet ($U \sim t^{-1}$). Examples of this third type include a February 1990 eruption of Lascar volcano in Chile; a July 1980 eruption of Mount St Helens in the Western US; and two eruptions of Soufrière Hills volcano (Figure 28.8).

For steady plume-forming eruptions, collapse and pyroclastic density current formation is favored for large vent radii, low vent velocities, and high solid mass fractions at the vent and for large particles. Examples of Vulcanian plumes that have collapsed and produced pyroclastic density currents include Mount St Helens during the summer of 1980 and Soufrière Hills volcano, Montserrat, in July, August, and September of 1997. The conditions that favor collapse are similar to, although more complex than, those for steady plumes. In particular, the rapidly changing vent conditions and the varied ways in which Vulcanian jets entrain atmospheric air play a significant role, and are not definitively characterized. Unsteady jets and plumes are

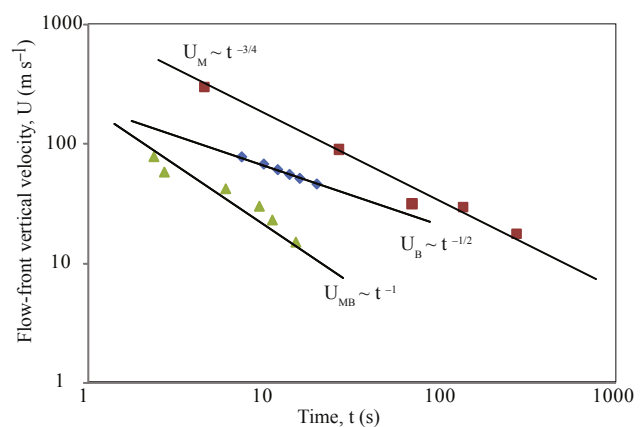


FIGURE 28.8 Vertical flow front velocity vs. time for three different Vulcanian eruptions. The 1975 eruption of Ngauruhoe (New Zealand) was dominated by momentum M as shown by the relationship $U \sim t^{-3/4}$ (squares). The 1982 eruption of Sakurajima (Japan) was dominated by buoyancy B (thermal) as shown by the relationship $U \sim t^{-1/2}$ (diamonds). The August 7, 1997 eruption of Soufrière Hills volcano (Montserrat, British West Indies), was controlled by both momentum M and buoyancy B , as shown by the relationship $U \sim t^{-1}$ (triangles). Modified from Clarke et al. (2009).

thought to entrain atmospheric air at different rates with respect to their well-documented steady equivalents; entrainment in Vulcanian jets and plumes depends on the temporal evolution of large-scale eddies and may be a function of local flow conditions, which rapidly change in time and space. These complexities are important because column collapse is in part controlled by entrainment, especially in the near-vent region.

Additional complexities exist, causing natural Vulcanian events to vary to some extent from idealized models. Detailed analysis of the 1997 Vulcanian eruptions of Soufrière Hills volcano reveals that explosion initiation involves multiple, individual finger jets that have distinct characteristics and progressively increasing velocities. These observations indicate that there were preexplosive gradients in volatiles in the shallow conduit, and that fragmentation, especially in the initial stages, was heterogeneous in time and space. Corresponding rates of

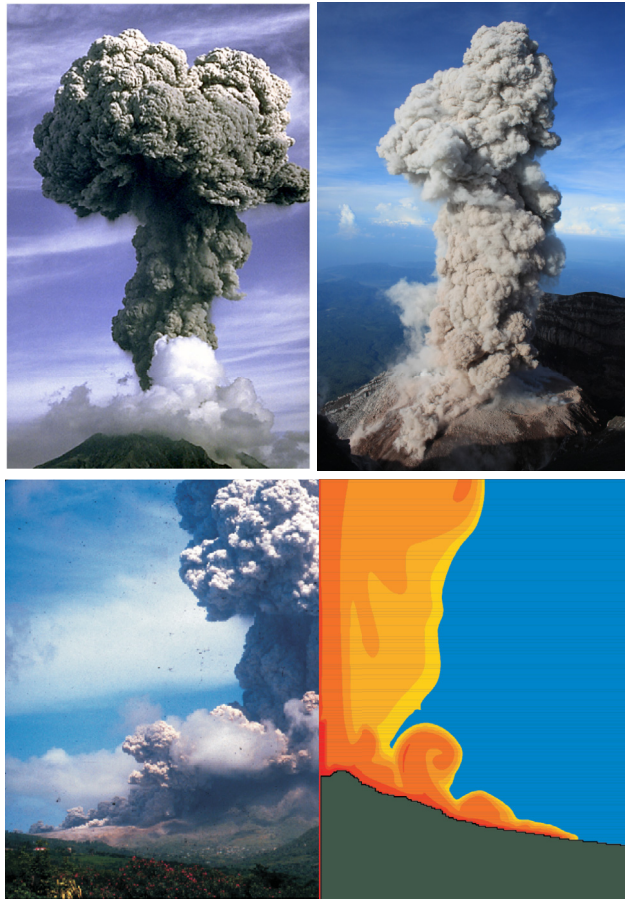


FIGURE 28.9 Images of the typical morphology of Vulcanian eruptions, as seen at Sakurajima volcano, Japan, (top left, Smithsonian Institution image), Semeru volcano, Indonesia (top right image, photo by Jean-Francois Smekens), and Soufrière Hills volcano, Montserrat (bottom). The image of Soufrière Hills eruption is a hybrid of a photograph by B. Voight and multiphase numerical simulations of the event, the same simulations as represented in Figure 28.7.

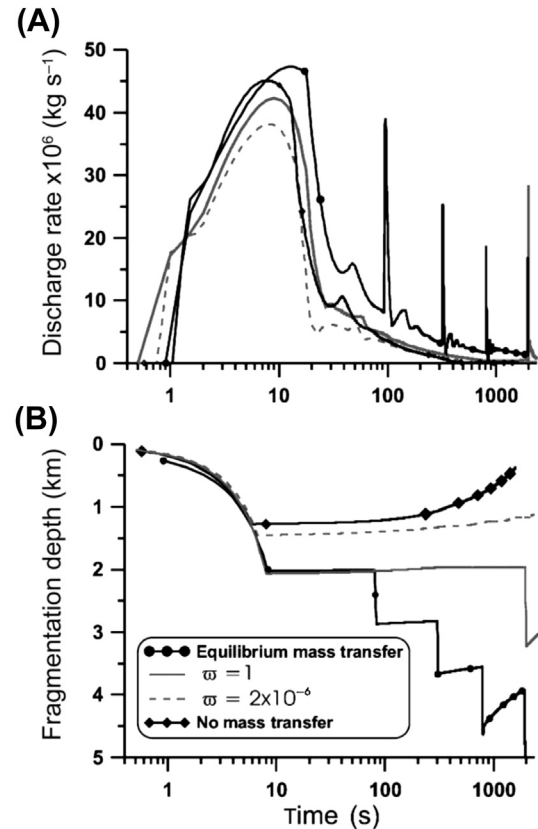


FIGURE 28.10 Calculated variation in discharge rate (A) and fragmentation front position (B) with time using the overpressured bubble fragmentation criterion. The system behaves differently depending on the effective rate of mass transfer of gas from the dissolved phase to the gas phase (rate of gas exsolution). As end members, the cases of no volatile mass transfer (Peclet number much greater than 1) and equilibrium mass transfer (Peclet number much less than 1) are shown, along with two intermediate cases expressed in terms of a gas diffusion factor which scales with gas diffusion rate and bubble number density. Note that the equilibrium volatile mass transfer case favors repeated pulses. Modified from Melnik and Sparks (2002).

entrainment of atmospheric air are very low for individual jets, and this inefficient entrainment is thought to have contributed to collapse and pyroclastic flow formation.

Two-dimensional (axisymmetric) modeling and numerical simulations of Vulcanian explosions at Soufrière Hills volcano (Figure 28.10) have shown that, for the most intense events, initial rapid expansion and the subsequent sudden decrease of mass flow rate generate complex collapse patterns qualitatively and quantitatively consistent with observed plume and PDC morphology.

12. CYCLIC ACTIVITY, TRANSITIONS IN ERUPTION STYLE

Vulcanian eruptions may transform into sustained, quasi-steady explosive eruptions or may end suddenly to be replaced by effusive dome building. Due to their evolved

magma compositions, it is reasonable to assume that gas does not diffuse from the melt into bubbles during propagation of the fragmentation front into the conduit. However, when volatile diffusion is fast and efficient, such as for high bubble number densities and high volatile diffusion rates, this assumption becomes invalid. The role of syn-fragmentation gas exsolution can be determined by examining the Peclet number (Pe), which is the ratio of the timescale for gas exsolution to the timescale of fragmentation.

The timescale of exsolution is determined by the rate of diffusion of a volatile in the melt and the length scale in question. This timescale is a function of bubble number density and the diffusion coefficient of gases (mainly water) in the melt. End members are zero gas exsolution and the equilibrium case in which gas exsolution instantaneously responds to decompression. The timescale of fragmentation is a function of the distance between the decompression wave and the fragmentation front and the velocity of the fragmentation front relative to the (possibly) ascending unfragmented magma; this relative velocity is simply the difference between the two velocity vectors. When volatile diffusion is slow or the fragmentation front closely follows the decompression wave (fast fragmentation), the Peclet number is much greater than 1, and syn-fragmentation gas exsolution can be ignored. When volatile diffusion is fast or the fragmentation front lags the decompression wave (slow fragmentation), the Peclet number is much less than 1, and syn-fragmentation gas exsolution must be considered. For example, fragmentation velocity tends to increase when the initial pressure ratio and gas fraction in the conduit increase, while diffusion rate tends to increase when melt viscosity decreases (e.g., diffusion is faster in andesites than in dacites) and when volatile concentrations are higher.

However, because of complex, competing relationships, the expected outcome for a given system cannot be easily predicted. In order to explore the relationships more thoroughly, the system has been represented by conservation equations for a multicomponent magma rising in a one-dimensional conduit, accounting for the difference in pressure between the bubbles and the magma, gas exsolution during fragmentation depending on Peclet number, and crystallization. For these cases, numerical solutions have been used to explore the effects of syn-explosion gas diffusion on eruption characteristics. Model solutions show that no gas exsolution during fragmentation results in a single short-lived explosive pulse, which does not repeat until magma slowly ascends in response to conduit evacuation and prepares for another explosion. The equilibrium case results in repeated pulsatory eruptions (Figure 28.9); greater total volatile content for a given set of conditions pushes the system toward multiple pulses or quasi-steady behavior. The addition of crystals tends to increase the depth to which the fragmentation front reaches for a single pulse because of increased viscosity. However, magmas with

low crystal fractions and relatively low viscosities, are more likely to stabilize into a steady-state eruption because the magma will more easily ascend to meet and feed the fragmentation wave.

The choice of fragmentation criterion in magma ascent models does not significantly affect numerical results at the vent. However, strain rate and overpressure criteria are able to produce pulsatory behavior, whereas the volume fraction criterion tends to produce a single pulse. Moreover, maximum calculated fragmentation front velocities exceed 200 m s^{-1} for the first two criteria and are less than 50 m s^{-1} for the volume fraction criterion. Finally, transition from periodic explosions to effusive activity may occur when permeability, rather than fragmentation, develops either throughout the magma or along conduit walls, and therefore suppresses explosivity. A sequence of periodic explosive eruptions at Soufrière Hills volcano in 2003 is thought to have ended in this way via permeable escape of gas along conduit walls.

13. SUMMARY AND FUTURE PERSPECTIVES

A large variety of explosive volcanic phenomena fall under the category of Vulcanian eruptions. Their unpredictable (and hazardous) nature is related to the wide variability in the magma composition, volatile content, degassing and crystallization patterns (in space and time), and different preruptive distribution of vesicularity and pressure, all of which control magma decompression in the feeding conduit or dike, leading to different textural features in the resulting deposits. However, Vulcanian eruptions are well defined by their eruption mechanism, by means of which we can explain most of the features of their deposits and those commonly observed during eruption. Laboratory experiments and numerical models represent valuable tools for elucidating complex nonlinear processes and identifying their scaling properties. Future research work will need to address, in particular, the problem of nonequilibrium processes related to syn-eruptive degassing and crystallization and the complex rheology of the mixture of melt, crystals, and bubbles involved in the process.

Nonetheless, the conditions sufficient to produce a transition from quiescent or effusive states to Vulcanian events are still extremely difficult to establish and the forecasting of new explosive events, even during periods of persistent activity, is challenging.

New promising multiparameter-monitoring techniques are being developed on active volcanoes. Their development in the next years will likely provide further constraints for theoretical and experimental investigations and for the forecasting of Vulcanian explosions and volcanic risk mitigation.

ACKNOWLEDGMENTS

Much of our understanding of Vulcanian eruptions was gained in the field and through interactions with collaborators. In particular we acknowledge the contributions by members of the Montserrat Volcano Observatory, as well as Tim Druitt, Barry Voight, Augusto Neri, Marina Belousova, and Jeffrey Johnson. This compilation was possible via generous support from the National Science Foundation (USA), the INGV-Pisa (Italy), and the Institute of Volcanology and Seismology (Russia).

FURTHER READING

- Alatorre-Ibargüengoitia, M.A., Scheu, B., Dingwell, D.B., 2011. Influence of the fragmentation process on the dynamics of Vulcanian eruptions: An experimental approach. *Earth Planet Sci. Lett.* 302 (1), 51–59.
- Alidibirov, M., Dingwell, D.B., 1996. Magma fragmentation by rapid decompression. *Nature* 380 (6570), 146–148.
- Alidibirov, M.A., 1994. A model for viscous magma fragmentation during volcanic blasts. *Bull. Volcanol.* 56 (6–7), 459–465.
- Belousov, A., Belousova, M., 2001. Eruptive process, effects and deposits of the 1996 and ancient basaltic phreatomagmatic eruptions in Karymskoye lake, Kamchatka, Russia. In: White, J.D., Riggs, N.R. (Eds.), *Lacustrine Volcanoclastic Sedimentation*, IAS Special Volume, 30, pp. 235–260.
- Braitseva, O.A., Melekestsev, I.V., 1991. Eruptive history of Karymsky volcano, Kamchatka, USSR, based on tephra stratigraphy and C14 dating. *Bull. Volcanol.* 53, 195–206.
- Cas, R.A.F., Wright, J.V., 1987. *Volcanic Successions: Modern and Ancient*. Allen & Unwin, London, Boston, Sydney, Wellington xviii + 528.
- Chojnicki, K.N., Clarke, A.B., Phillips, J.C., 2006. A shock-tube investigation of the dynamics of gas-particle mixtures: Implications for explosive volcanic eruptions. *Geophys. Res. Lett.* 33 (15).
- Chojnicki, K.N., Clarke, A.B., Adrian, R.J., Phillips, J.C., 2014. The flow structure of jets from transient sources and implications for modeling short-duration explosive volcanic eruptions. *Geochem. Geophys. Geosyst.* 15, 4831–4845. <http://dx.doi.org/10.1002/2014GC005471>.
- Chojnicki, K.N., Clarke, A.B., Phillips, J.C., Adrian, R.J., 2014. Rise dynamics of unsteady laboratory jets with implications for volcanic plumes. *Earth and Planet. Sci. Lett.* 412, 186–196.
- Clarke, A.B., Phillips, J.C., Chojnicki, K.N., 2009. An investigation of Vulcanian eruption dynamics using laboratory analogue experiments and scaling analysis. *Stud. Volcanol.* 2, 155–166.
- Clarke, A.B., Voight, B., Neri, A., Macedonio, G., 2002. Transient dynamics of vulcanian explosions and column collapse. *Nature* 415 (6874), 897–901.
- Clarke, A.B., Neri, A., Macedonio, G., Voight, B., Druitt, T.H., 2002b. Computational modelling of the transient dynamics of the August 1997 Vulcanian explosions at Soufrière Hills volcano, Montserrat: influence of initial conduit conditions on near-vent pyroclastic dispersal. In: Druitt, T.H., Kokelaar, B.P. (Eds.), *The eruption of Soufrière Hills Volcano, Montserrat, from 1995 to 1999*, Geological Society, 21. Memoir, London, pp. 319–348.
- Clarke, A.B., Stephens, S., Teasdale, R., Sparks, R.S.J., Diller, K., 2007. Petrological constraints on the decompression history of magma prior to Vulcanian explosions at the Soufrière Hills volcano, Montserrat. *J. Volcanol. Geotherm. Res.* 161, 261–274.
- de' Michieli Vitturi, M., Neri, A., Esposti Ongaro, T., Lo Savio, S., Boschi, E., 2010. Lagrangian modeling of large volcanic particles: Application to Vulcanian explosions. *J. Geophys. Res.* 115, B08206. <http://dx.doi.org/10.1029/2009JB007111>.
- Druitt, T.H., Young, S.R., Baptie, B., Bonadonna, C., Calder, E.S., Clarke, A.B., Voight, B., 2002. Episodes of cyclic Vulcanian explosive activity with fountain collapse at Soufrière Hills Volcano, Montserrat. *Memoirs-Geol. Soc. London* 21, 281–306.
- Edmonds, M., Herd, R.A., 2007. A volcanic degassing event at the explosive-effusive transition. *Geophys. Res. Lett.* 34 (21).
- Formenti, Y., Druitt, T.H., Kelfoun, K., 2003. Characterisation of the 1997 Vulcanian explosions of Soufrière Hills Volcano, Montserrat, by video analysis. *Bull. Volcanol.* 65 (8), 587–605.
- Ishihara, K., 1985. Dynamical analysis of volcanic explosion. *J. Geodyn.* 3 (3), 327–349.
- Johnson, J.B., Lees, J.M., 2000. Plugs and chugs—seismic and acoustic observations of degassing explosions at Karymsky, Russia and Sangay, Ecuador. *J. Volcanol. Geotherm. Res.* 101, 67–82.
- Lopez, T., Fee, D., Prata, F., Dehn, J., 2013. Characterization and interpretation of volcanic activity at Karymsky Volcano, Kamchatka, Russia, using observations of infrasound, volcanic emissions, and thermal imagery. *Geochem. Geophys. Geosyst.* 14, 5106–5127.
- Mason, R.M., Starostin, A.B., Melnik, O.E., Sparks, R.S.J., 2006. From Vulcanian explosions to sustained explosive eruptions: the role of diffusive mass transfer in conduit flow dynamics. *J. volcanol. geotherm. res.* 153 (1), 148–165.
- Melnik, O., Sparks, R.S.J., 2002. Modelling of conduit flow dynamics during explosive activity at Soufrière Hills Volcano, Montserrat. In: Druitt, T.H., Kokelaar, B.P. (Eds.), *The Eruption of Soufrière Hills Volcano, Montserrat, from 1995 to 1999*, Geol. Soc. vol. 21. Mem. London, pp. 307–317.
- Morrissey, M., Garces, M., Ishihara, K., Iguchi, M., 2008. Analysis of infrasonic and seismic events related to the 1998 Vulcanian eruption at Sakurajima. *J. Volcanol. Geotherm. Res.* 175 (3), 315–324.
- Morrissey, Mastin, 1999. Vulcanian eruptions. In: Sigurdsson, H., Houghton, B., Rymer, H., Stix, J., McNutt, S. (Eds.), *Encyclopedia of Volcanoes*. Academic Press.
- Mueller, S., Scheu, B., Spieler, O., Dingwell, D.B., 2008. Permeability control on magma fragmentation. *Geology* 36 (5), 399–402.
- Orescanin, M.M., Austin, J.M., Kieffer, S.W., 2010. Unsteady high-pressure flow experiments with applications to explosive volcanic eruptions. *J. Geophys. Res.* 115 (B6), B06206.
- Self, S., Wilson, L., Nairn, I.A., 1979. Vulcanian eruption mechanisms. *Nature* 277, 440–443.
- Siebert, L., Simkin, T., 2002. *Volcanoes of the World: An Illustrated Catalog of Holocene Volcanoes and their Eruptions*. Global Volcanism Program Digital Information Series GVP-3. Smithsonian Institution.
- Spieler, O., Kennedy, B., Kueppers, U., Dingwell, D.B., Scheu, B., Taddeucci, J., 2004b. The fragmentation threshold of pyroclastic rocks. *Earth Planet. Sci. Lett.* 226 (1–2), 139–148.
- Walker, G.P.L., 1973. Explosive volcanic eruptions — a new classification scheme. *Geol. Rundsch.* 62 (2), 431–446.
- Woods, A.W., Sparks, R.S.J., Ritchie, L.J., Batey, J., Gladstone, C., Bursik, M.I., 2002. The explosive decompression of a pressurized volcanic dome: the 26 December 1997 collapse and explosion of Soufrière Hills Volcano, Montserrat. *Geol. Soc., London, Memoirs* 21 (1), 457–465.
- Woods, A.W., 1995. A model of Vulcanian eruptions. *Nucl. Eng. Des.* 155, 345–357.
- Wright, J.V., Smith, A.L., Self, S., 1980. A working terminology of pyroclastic deposits. *J. Volcanol. Geotherm. Res.* 8, 316–336.